Two-State Folding of Horse Ferrocytochrome *c*: Analyses of Linear Free Energy Relationship, Chevron Curvature, and Stopped-Flow Burst Relaxation Kinetics†

Rajesh Kumar and Abani K. Bhuyan*

School of Chemistry, University of Hyderabad, Hyderabad 500046, India

Received September 27, 2004; Revised Manuscript Received November 21, 2004

ABSTRACT: Ferrocytchrome *c* is a classic two-state fast folder. This assurance comes from extensive equilibrium and kinetic folding studies carried out under strictly anaerobic conditions at 22 °C. Conventional guanidine hydrochloride (GdnHCl)-induced unfolding transitions monitored by the use of a sizable set of optical probes do not reveal the accumulation of any intermediate to a detectable level. The GdnHCl dependence of unfolding free energy (ΔG_D) is linear over the full range of the denaturant concentration. The GdnHCl folding chevron is characterized by curvatures in both folding and unfolding limbs. However, refolding rates as a function of urea in the presence of different concentrations of GdnHCl yield $m_f^{\ddagger}$ values (the kinetic *m*-value) that are quantitatively identical. This result, analyzed in terms of the denaturant dependence of the difference in the extent of solvent exposure between a relatively fixed transition state and the preceding state involved in the transition, suggests that the chevron curvature is not related to differential accumulation of a folding intermediate with varying concentration of GdnHCl in the refolding medium. Denaturant dependence of stopped-flow burst signals recorded in normal refolding experiments (pH 7, 22 °C) is essentially identical with that recorded in simulating experiments in which the protein stays steadily unfolded even in the denaturant-diluted medium (pH 1.5−2, 22 or 43 °C depending on the use of urea or GdnHCl), and they match the denaturant dependence of equilibrium signals for the unfolded protein. The results demonstrate that the burst phase does not entail an early folding intermediate. Rather, the folding kinetics are essentially two-state. These results are central to the phenomenological description of protein folding.

Ever since the pioneering work of Tanford and co-workers (*1*) and others (*2*−*4*), horse cytochrome *c* (cyt *c*)[1] has served as a paradigm in the pursuit of the protein folding code. Indeed, some of the fundamental concepts in this area have evolved from extensive work with ferricyt *c* (*5*−*8*, and refs therein). There have, however, been serious problems from the viewpoint of interpretation of results, most of the conflicts arising from undesirable modulations in heme−polypeptide contacts across the folding−unfolding equilibrium. The chemistry involved is very well understood (*6*, *9*−*12*). Briefly, the native-state axial ligation of M80 to the oxidized heme is replaced by H26 and H33 under destabilizing conditions. Even though non-native, the Fe^{3+}−H26 and Fe^{3+}−H33 contacts are stable, and therefore the dissociation rates of these two ligands from the iron are far smaller than the protein folding rate. Consequently, the polypeptide collapses with persisting Fe^{3+}−H26 and Fe^{3+}−H33 contacts. This act of misfolding generates chain misconfiguration at later stages of folding. Folding is then retarded because the frustrated chain organization stays in a kinetically frozen intermediate state until thermal dissociation of non-native histidines from the heme iron gives way to the ligation of M80, thus facilitating polypeptide reconfiguration. Such fortuitous events not only obscure the processes that are of fundamental interest but also lead to subtly conflicting interpretations. For example, to achieve correct chain configuration at a later stage of folding, an unfolding event that would disperse the incorrect organization is necessary. In this sense, the intermediate could be regarded as a trapped misfolded intermediate (*10*), a prototype of late intermediates predicted by theoretical studies (*13*). On the other hand, the intermediate may be described just at the level of the relevant N- and C-terminal helices without paying any attention to wrong chain organizations in other parts of the molecule (*11*, *14*). The problem of kinetic trap or chain misorganization in the folding run of ferricyt *c* can be mitigated by allowing refolding at low pH or in the presence of an extrinsic heme ligand that blocks non-native histidine ligation. Folding kinetics are then modeled as a two-state reaction (*7*, *15*) or by invoking intermediates (*5*), again a matter of conflict.

Interpretational ambiguities are avoided with ferrocytochrome *c* (ferrocyt *c*), since non-native heme ligands do not interfere with inherent accelerated folding of this redox state of cyt *c*. Aqueous stability of ferrocyt *c* is extremely high (∼18 kcal mol^{-1} at 22 °C), and stopped-flow observable millisecond kinetics are fast, simple, and essentially monopha-

† This work was supported by grants from Department of Biotechnology (BRB/15/227/2001), Department of Science and Technology (4/1/2003-SF), and University Grants Commission (UPE Funding), Government of India.

* To whom correspondence should be addressed. E-mail: akbsc@uohyd.ernet.in. Fax: 91-40-23012460.

[1] Abbreviations: GdnHCl, guanidine hydrochloride; ΔG_D, Gibbs energy of denaturation; ΔG_D°, Gibbs energy of denaturation in the absence of denaturant; cyt *c*, cytochrome *c*; ferricyt *c*, ferricytochrome *c*; ferrocyt *c*, ferrocytochrome *c*; CD, circular dichroism.

10.1021/bi0478998 CCC: $30.25
Published on Web 02/01/2005

sic (*12*, *16*−*18*). These virtues render ferrocyt *c* even more attractive a system for exploring the fundamental principles that govern protein folding (*17*).

Studies have projected ferrocyt *c* as a prototype of a two-state protein (*12*, *16*, *17*). A very recent paper, however, states that folding of ferrocyt *c* is not two-state (*19*). Despite the simplicity of observed folding kinetics, the rates roll over in the folding chevron of ferrocyt *c* (*12*). Further, a submillisecond burst change in optical signals characterizes the stopped-flow kinetics (*17*). These two criteria would appear to disqualify ferrocyt *c* for a two-state system, since one of the interpretations of chevron curvature is that accumulation of an early intermediate, presumably formed in the burst phase, limits the overall rate of refolding (*20*−*22*). The phenomenon of chevron curvature coupled with burst signals, observed for a number of proteins, is often used as a strong evidence for a general three-state (or even higher) protein folding mechanism (*22*−*24*, for example). But careful studies have also shown that a number of small proteins, folding kinetics of which were earlier described as three-state on the basis of observed chevron curvature and submillisecond burst kinetics, are actually two-state (*25*−*29*).

To demonstrate further that the folding kinetics of ferrocyt *c* are indeed two-state, despite the observed chevron curvature and burst kinetics, this paper presents results of some basic equilibrium and kinetic folding experiments. Since kinetic intermediates are best described when equilibrium experiments hint at their accumulation, an exhaustive search for a neutral-pH equilibrium intermediate was made. Transitions probed by the use of circular dichroism at several wavelengths ranging from far-UV to the near-infrared region, heme absorbance at Soret, visible, and near-infrared bands, and heme-tryptophan fluorescence excitation energy transfer, are all coincident and two-state. Kinetic experiments, in which refolding in the presence of different concentrations of GdnHCl along the chevron were measured as a function of urea, indicate that the chevron curvature is not due to the accumulation of a kinetic intermediate. Analyses of GdnHCl and urea distributions of burst relaxation signals of persisting unfolded cyt *c* at pH 1.5−2 and normal cyt *c* at pH 7 suggest that the submillisecond burst phase does not entail a structural intermediate.

These demonstrations are essential to be able to use ferrocyt *c* kinetics for a mechanistic description of protein folding given in the companion article in this issue (*30*).

MATERIALS AND METHODS

Horse heart cyt *c* (Type VI) was from Sigma. Denaturants were obtained from Gibco BRL. Other chemicals were analytical grade. All experiments were done in 0.1 M sodium phosphate buffer at 22 °C unless indicated otherwise. Extreme care was taken to avoid air exposure of solutions at all stages of experiments.

Measurements of Equilibrium Unfolding. The protein concentration varied from 8 μM to 2.1 mM depending on the transition dipole strength of the spectroscopic probe used. Stock solutions of the native and the unfolded protein (6−8 M GdnHCl or 10 M urea) were mixed appropriately to obtain protein samples containing different concentrations of denaturants. To prepare ferrocyt *c*, solutions were exhaustively deaerated under argon or nitrogen before addition of a small volume of a concentrated aqueous solution of sodium dithionite to obtain a final reductant concentration of 1−3 mM. The sample was sealed under argon and equilibrated for ~45 min at 22 (±1) °C. The process of sample reduction caused little inconsistency in the protein concentration from one sample to another. pH and denaturant concentrations of samples were checked before and after measurements. The reported GdnHCl concentrations are those determined after taking data.

Fluorescence spectra were recorded in a photon counting instrument (FluoroMax-3, Jobin-Yvon). Optical absorption measurements were done using a Cary 100 (Varian) or a Shimadzu UV-3101PC spectrophotometer. For CD measurements, a JASCO J715 instrument was used. Corrections for buffer signal, including the contribution of denaturants, were done routinely.

Measurement and Primary Analysis of Folding−*Unfolding Kinetics*. The procedure for kinetic experiments under controlled anaerobic conditions has been described earlier (*16*). Cyt *c* initially unfolded in 6.5 M GdnHCl, pH 7, was reduced under nitrogen by adding a concentrated solution of sodium dithionite to a final concentration of ~3 mM. The final protein concentration in the refolding mixture was 44 μM when experiments involved GdnHCl alone. The final protein concentration for those experiments where refolding was carried out in the presence of various concentrations of urea was 16 μM. Use of the same protein concentration in all experiments involving urea facilitated data normalization. Unfolding experiments involved only GdnHCl and were performed following the same procedure of two-syringe mixing. The final protein concentration in unfolding experiments was ~28 μM. Kinetics were measured at 22 °C under strictly anaerobic conditions. Gastight syringes were employed to transfer protein and buffer solutions into stopped-flow syringes. A SFM 400 mixing module (Biologic) was used. Excitation wavelength was 280 nm, and emission was measured using a 335 nm cutoff filter. Typically, 10−20 shots were averaged.

Kinetic traces were analyzed using single- or double-exponential functions to extract apparent rates, λ_i, the initial signal, S_o, which corresponds to the "zero-time" signal in the stopped-flow time window, the observed signal, S_{obs}, and the final equilibrium signal, S_∞, corresponding to the signal value at $t = t_\infty$. The S_o, S_{obs}, and S_∞ signals were subjected to initial normalization by first subtracting the buffer fluorescence signals, and then dividing by the recorded signal of the unfolded protein in the highest GdnHCl concentration. In the unfolding set of measurements the S_∞ value of the kinetic trace at the highest concentration of GdnHCl employed was used to divide the fluorescence signals.

RESULTS

Two-State Equilibrium Unfolding. In search of equilibrium population of structural intermediates of ferrocyt *c*, the GdnHCl-induced unfolding transition was probed by employing CD at several wavelengths in the far-UV to the near-infrared region, heme absorbance at Soret, visible and near-infrared bands, and tryptophan fluorescence (Figure 1). Since optical properties of different spectroscopic probes are different in both pre- and posttransition regimes, the unfold-

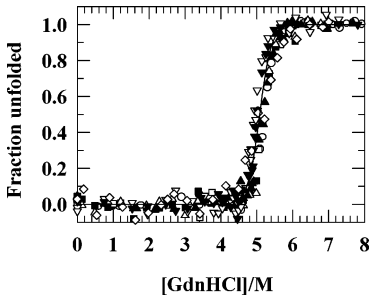

FIGURE 1: Plots of fraction of ferrocyt *c* unfolded as a function of GdnHCl probed by CD signals at 222 nm (○), 290 nm (●), 413 nm (□), 525 nm (■), and 603 nm (△), tryptophan fluorescence at 358 nm (▲), and heme absorption at 430 nm (▽), 549 nm (▼), and 643 nm (◇). The origins of these optical transitions are well understood. The 643-nm band associated with the unfolding of ferrocyt *c* has not been described before. The solid line represents the iterated least-squares fit of the data to a two-state unfolding transition. The fit yields $\Delta G_D^\circ = 17.9$ (±1) kcal mol^{-1} and $m_g = 3.54$ (±0.05) kcal mol^{-1} M^{-1}. All transitions were measured at 22 (±1) °C, 0.1 M phosphate, pH 7.

ing curves shown were normalized individually according to the observed functional dependence of the optical property on GdnHCl. The pre- and post-unfolding baselines in the raw data were fitted to first-order polynomial to extract normalized values of fraction unfolded as a function of the denaturant. Figure 1 shows the simple result that the transitions measured by different optical probes are, within error, nearly superimposable and cooperative. The observation of indistinct transition curves fails the basic test for accumulation of equilibrium intermediate to a detectable level.

The solid line in Figure 1 is a two-state fit of the data assuming a linear functional dependence of ΔG on GdnHCl according to refs *31* and *32*.

$$\Delta G_D = \Delta G_D^\circ - m_g[\text{GdnHCl}] = m_g(C_m - [\text{GdnHCl}]) \quad (1)$$

where ΔG_D° is the free energy of unfolding in the absence of denaturant, m_g (= $2.3RT\ \partial\log K/\partial[\text{GdnHCl}]$); the subscript "g" in m_g stands for global) is a parameter related to the change in surface area in global unfolding of the protein, and C_m is the GdnHCl concentration at which $\Delta G_D = 0$. Values of ΔG_D° and m_g obtained from this analysis are 17.9 (±1) kcal mol^{-1} and 3.54 (±0.05) kcal mol^{-1} M^{-1}, respectively, indicating enormous aqueous stability of ferrocyt *c*.

The equilibrium parameters for the unfolding of ferrocyt *c* are independent of protein concentration. In the present study, the protein concentration used for various spectroscopic probes differed widely, in the 0.008−2.1 mM range. Despite a 260-fold difference in the protein concentration the two-state unfolding parameters did not change. The coincidence of various transition curves for different protein concentrations provides a reason to rule out the possible accumulation of associating intermediates of the kind reported for certain solvent-induced unfolding of proteins (*33*, *34*).

Dependence of the Free Energy of Unfolding, ΔG, on GdnHCl. But how reliable is the value of ΔG_D°? A simple approach to validate the linear extrapolation method is to analyze unfolding transitions induced by one denaturant in the presence of several lower concentrations of another (*35*). The strategy used in this study is to extract ΔG_D° values

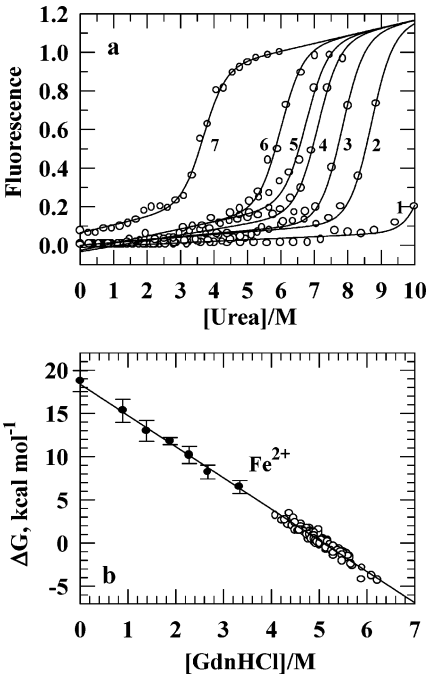

FIGURE 2: (a) Urea-induced denaturation of ferrocyt *c* in the presence of different concentrations of GdnHCl, 22 (±1) °C, 0.1 M phosphate, pH 7. Curve labels 1 to 7 correspond to 0, 0.9, 1.4, 1.9, 2.3, 2.7, and 3.35 M GdnHCl, respectively. Values of ΔG_D° (in kcal mol^{-1}) for curves 7 to 1 are 6.49 (±0.75), 10.54 (±0.8), 11.87 (±1.0), 12.49 (±0.4), 13.77 (±1.2), 15.29 (±1.33), and 18.73 (±1.21), respectively. The value of 1.76 (±0.4) kcal mol^{-1} M^{-1} for m_g, obtained from the fit to curve 7 (eq 2), was used to constrain the fits to curves 1−6 (see text). (b) Plot of ΔG_D (○, extracted from data in Figure 1) and ΔG_D° (●, determined from curves 1−7 shown in panel a) as a function of GdnHCl. Values of ΔG_D° and m_g, obtained as the *y*-intercept and the slope of the linear least-squares fit ($r = 0.99$), are 18.36 (±0.45) kcal mol^{-1}, and 3.61 kcal mol^{-1} M^{-1}, respectively.

from a series of urea-induced unfolding transitions, one transition in the presence of a given GdnHCl concentration, and then to test if they are mapped linearly onto the ΔG_D values already obtained from the data shown in Figure 1. Therefore, urea-induced transition curves of ferrocyt *c* in the presence of 0, 0.9, 1.4, 1.9, 2.3, 2.7, and 3.3 M GdnHCl were recorded under identical conditions of pH and temperature. Figure 2a shows these data. It is clear that within the limit of the aqueous solubility of urea, complete unfolding is achieved only in the presence of 3.3 M GdnHCl. Observation of incomplete unfolding in the presence of other concentrations of GdnHCl is not surprising, given the extraordinary thermodynamic stability of ferrocyt *c*. To make progress, all data sets were normalized with respect to the fluorescence observed in 6 M urea and 3.3 M GdnHCl (i.e, the last point in the transition labeled 7). Transition 7, which shows complete unfolding, was then analyzed using eq 2 (*36*).

$$S_{obs} = \frac{(c_f + m_f[\text{D}]) + (c_u + m_u[\text{D}])\exp\left(\dfrac{-\Delta G_D^\circ + m_g[\text{D}]}{RT}\right)}{1 + \exp\left(\dfrac{-\Delta G_D^\circ + m_g[\text{D}]}{RT}\right)} \quad (2)$$

where S_{obs} is the observed signal, c_f and c_u, and m_f and m_u represent intercepts and slopes of native and unfolded

baselines, respectively, and D represents urea concentration. All parameters were floated during fitting. The iterated fit parameters are given in the legend to Figure 2. Since the urea dependence of post-unfolding baselines is expected to be same for all transitions, the values of c_u and m_u obtained from the analysis of transition 7 can be used to constrain the fits to transitions 1−6. To search for other constraints, the same series of experiments was repeated with ferricyt *c* (data not shown). Because of its lower stability ($\Delta\Delta G^\circ_D = 8$ (±1) kcal mol^{-1}) ferricyt *c* is completely unfolded by urea even in the absence of GdnHCl. Analysis of these data (not shown) indicated that the value of m_g (1.7 (±0.06) kcal mol^{-1} M^{-1}) does not vary at all with different concentrations of GdnHCl in the unfolding medium, consistent with results of similar studies reported earlier (*35*). This observation provided a basis for constraining the value of m_g in the analysis of ferrocyt *c* unfolding curves. Hence, values of c_u, m_u, and m_g determined from transition 7 were used in eq 2 to constrain the fits to transitions 1−6. Thermodynamic parameters thus obtained are given in the legend to Figure 2.

To test the validity of linear functional dependence of Gibbs free energy of unfolding on GdnHCl, the values of ΔG_D determined from urea unfolding curves are plotted in Figure 2b together with the values of ΔG_D ($= -RT \ln K$) calculated from the curves shown in Figure 1. A linear least-squares fit of the data ($r = 0.99$) yields $\Delta G^\circ_D = 18.36$ (±0.45) kcal mol^{-1} and $m_g = -3.6$ kcal mol^{-1} M^{-1}. These values of ΔG°_D and m_g are in excellent agreement with those obtained from the equilibrium curves shown in Figure 1. The results thus validate the linear functional dependence of ΔG_D on GdnHCl in the full range of the denaturant concentration.

The Curvatures in Folding Chevron and Burst Relaxation. Stopped-flow kinetics of the folding−unfolding reaction of ferrocyt *c* were recorded as a function of GdnHCl to check for possible accumulation of kinetic intermediate. For refolding, ferrocyt *c* was initially unfolded in 6.5 M GdnHCl, pH 7. Figure 3a shows the initial 100 ms of a representative kinetic trace that is best described by two exponentials: a major phase ($k_{obs} = 276$ s^{-1}) and a minor phase ($k_{obs} = 39$ s^{-1}). The slow minor phase, the amplitude of which averages to no more than 10 (±2)% of the total observed amplitude, is due most likely to a small heterogeneous population and is excluded from further analysis. The kinetic trace also reports on the loss of 70% of the total expected fluorescence in a burst refolding phase that is complete within the dead time of the stopped flow (~2.6 ms).

Figure 3b shows the denaturant dependence of the logarithm of the observed folding and unfolding rates. The relaxation minimum in the chevron plot corresponds to the transition midpoint ($C_m \approx 5$ M GdnHCl, see Figure 1). The observed folding rate increases progressively as the GdnHCl concentration in the refolding medium is lowered below the transition midpoint. The rate-denaturant relationship is apparently not linear; however, the rates roll over as increasingly nativelike conditions are approached. Similar rollover of unfolding rates is observed as strongly unfolding conditions are approached. This is atypical of a kinetically two-state protein, especially when the dependence of ΔG_D on GdnHCl has been found to be linear (Figure 2b). To account for curvatures in both folding and unfolding limbs the chevron is fitted within the constraint of a two-state N ⇌ U

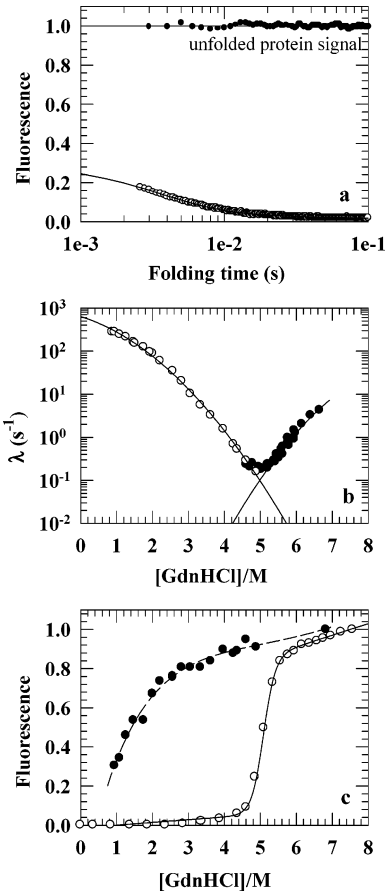

FIGURE 3: (a) Refolding trace in the presence of 0.95 M GdnHCl, 0.1 M phosphate, 22 °C. The amplitude is normalized with reference to the fluorescence of the unfolded protein (6.8 M GdnHCl). A prominent burst amplitude (70%) is apparent. Kinetics are best described by two exponentials: 276 s^{-1} (90% amplitude) and 39 s^{-1} (10% amplitude). The slower phase is due likely to heterogeneity or a small fraction of the oxidized protein in the unfolded sample. (b) The chevron: refolding (○) and unfolding (●). The solid lines are quadratic fits according to eq 3. (c) GdnHCl dependence of the burst amplitude. Solid circles are the normalized amplitude of the major kinetic phase. The broken line through these points is an empirical fit to $y = a + bx + cx(\exp(-dx))$, where *a*, *b*, *c*, *d* are constants. The equilibrium transition (○) yields $\Delta G^\circ_D = 17.99$ kcal mol^{-1} and $m_g = 3.54$ kcal mol^{-1} M^{-1}.

model by assuming the following quadratic relationship between log $k_{f(u)}$ and GdnHCl (*37*).

$$\log k_f = \log k^\circ_f - m_{1,f}[D] - m_{2,f}[D]^2$$
$$\log k_u = \log k^\circ_u + m_{1,u}[D] - m_{2,u}[D]^2 \quad (3)$$

An earlier interpretation of chevron curvature is the transient accumulation of kinetic intermediates (*20*, *21*). Under strongly nativelike conditions, where structural intermediates are expected to accumulate due to their increased stability, the observed refolding rate is limited by the rate of I → N conversion according to a U ⇌ I ⇌ N scheme.

The chevron rollover may appear coupled to burst refolding of ferrocyt *c*. Figure 3c shows the denaturant distribution of the normalized burst relaxation signals. The "zero-time" fluorescence signal in the stopped-flow time window (S_o), quantified by extrapolating the fitted kinetic traces to $t = 0$, decreases as the final GdnHCl concentration in the refolding medium is lowered. The area between the S_o values and the

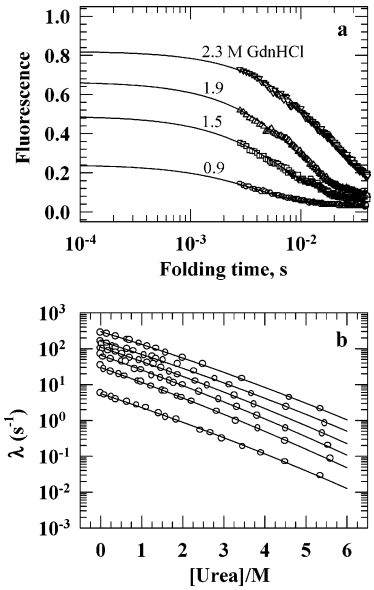

FIGURE 4: (a) Representative traces for refolding to 0.2 (±0.05) M urea in the presence of 0.9 (○), 1.5 (□), 1.9 (△) and 2.31 (▽) M GdnHCl. (b) k_f versus urea plots for refolding in the presence of (from top to bottom) 0.9, 1.5, 1.9, 2.3, 2.7, and 3.0 M GdnHCl.

equilibrium post-unfolding baseline extrapolated linearly to nativelike conditions contains the unobservable fluorescence changes associated with burst folding kinetics. Burst refolding is also seen in the folding kinetics of ferricyt *c*, and the GdnHCl dependence of the S_o values has often been assumed to be reminiscent of a distinct phase transition of a refolding intermediate that is fully formed within the dead time of stopped-flow (*14*). It may then appear that the rollover in the folding limb of ferrocytchrome chevron is also due to accumulation of an intermediate.

A Test on the Interpretation of Chevron Curvature. To test if the chevron rollover indeed originates from accumulation of a transient intermediate, an extended series of kinetic experiments was carried out in which refolding of ferrocyt *c* in the presence of 0.9, 1.5, 1.9, 2.3, 2.7, and 3.0 M GdnHCl was studied as a function of urea. The rationale is that if an intermediate is involved, and it is populated increasingly with more nativelike conditions, then the gradients of log k_f versus urea for different concentrations of GdnHCl in the refolding medium are not expected to be uniform.

Figure 4a samples the initial 40 ms of kinetic traces showing refolding of ferrocyt *c* to 0.2 (±0.05) M urea in the presence of GdnHCl concentrations indicated. The traces are described by single exponential, and they show the burst behavior discussed earlier. Figure 4b shows the plots of log k_f against urea for the six different concentrations of GdnHCl. While the lowest concentration of GdnHCl (0.9 M, the uppermost plot) offers a strongly nativelike condition in which the chevron curvature is accentuated (Figure 3b), the highest one (3.0 M, the lowermost plot) approaches the transition region where the protein is expected to operate in a two-state N ⇌ U manner. The relationship between log k_f and urea is not absolutely linear. The data are best described by

$$\log k_f = \log k_f^\circ - m_f[\text{urea}] - 0.0103[\text{urea}]^2 \qquad (4)$$

where $m_f^\ddagger = 2.303RT(m_f - 0.0103[\text{urea}])$. Note that the kinetic *m*-value under linear rate-denaturant assumption is given by $m_{f(u)}^\ddagger = 2.3RT\,\partial\log k_{f(u)}/\partial[\text{GdnHCl}])$.

The normalized quantity $\alpha = m_f^\ddagger/m_g$, where m_g is the change in surface area in urea-induced equilibrium unfolding, provides a measure of the amount of surface area buried upon folding from the initial denatured state to the transition state in a given concentration of GdnHCl. As the slopes of the plots suggest, the value of $m_f^\ddagger/m_g$ is found to be uniform for all the concentrations of GdnHCl used. At 2 M urea, for example, $m_f^\ddagger/m_g = 0.27$ (±0.02). This observation indicates that the initial denatured state that is created by rapid dilution of the unfolded protein is not a kinetic intermediate, and the chevron rollover is, therefore, not due to the accumulation of a kinetic intermediate under nativelike conditions.

Testing on the Origin of Urea Dependence of Burst Relaxation Signals. Since the ultrafast signals are associated with the incipient event in folding, it would be of interest to know if these optical signals are related to those that originate from the initial transient denatured states. Let the denatured state be the unfolded state under low denaturant (or refolding) conditions. The check requires finding conditions under which the protein is steadily unfolded even in the absence of a denaturant. One then compares the denaturant dependences of its equilibrium signal with the "zero time" burst signal under identical experimental conditions (*38*, *39*). In earlier experiments, a fragment of ferricyt *c* was used to model the unfolded protein (*38*). It is, however, desirable to use the whole protein rather than a fragment. The present study primarily deals with ferrocyt *c*. But because of its large stability no condition exists, not even at very high temperature, under which ferrocyt *c* is unfolded in the absence of high concentrations of denaturant. Experiments were therefore designed to investigate the denaturant dependence of burst relaxation signals of intact persistently unfolded ferricyt *c*.

U_A, the acid-unfolded state of ferricyt *c* (pH 1.5−2, without Cl^- ions), closely simulates the denaturant-unfolded state of the protein at pH 7 (*40*, *41*). Although assumed to be structureless, U_A shows some changes in tryptophan fluorescence when titrated with urea (Figure 5a). Nevertheless, U_A is truly structureless in urea concentrations > 2 M. Figure 5b presents a few kinetic traces to show what happens to the fluorescence of U_A when it is transferred rapidly from a solution of 10 M urea to ones of lower concentration of the denaturant in a stopped-flow. Each denaturant jump sets the fluorescence signal to a new value, S_o (signal at time $t = 0$), within the dead-time of the stopped flow, and the signal continues thereafter at the same level without any detectable change, S_∞ (the signal at time $t = \infty$). For all refolding jumps, $S_o = S_\infty$. In the presence of 0.8 M urea the reset value is ~60% less than the fluorescence of U_A in the presence of 10 M urea. To compare these results with those derivable from actual folding−unfolding reactions, equilibrium and kinetic experiments were conducted with ferricyt *c* at pH 7, 22 °C. Figure 5c maps the urea dependence of normalized values of burst and equilibrium signals for the U_A state (pH 1.5) onto those obtained from normal refolding experiments (pH 7). It is apparent that (i) the urea dependences of the two sets of burst signals overlap, (ii) urea distribution of both sets of burst signals are in agreement with that of the equilibrium fluorescence of the U_A state, and (iii) in higher

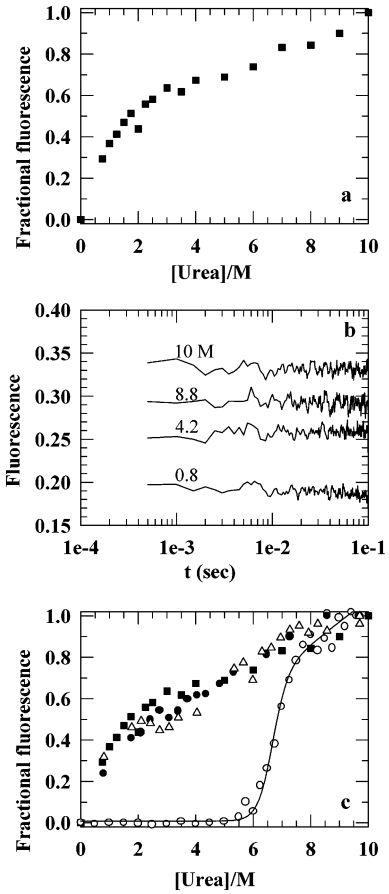

FIGURE 5: (a) Fluorescence of ferricyt *c* as a function of urea, pH 1.5, 22 °C. The fluorescence values were normalized by $(F_x - F_0)/(F_{10} - F_0)$, where F_x, F_0, and F_{10} are values in the presence of *x*, 0, and 10 M urea, respectively. (b) Typical time-resolved fluorescence signals of ferricyt *c* (pH 1.5, 22 °C) recorded by stopped-flow dilution of urea from 10 M to different final concentrations indicated. (c) Urea dependence of burst signals quantified from normal refolding kinetics at pH 7, 22 °C (●) is compared with burst signals recorded at pH 1.5 as shown in panel b (△), equilibrium fluorescence signals of cyt *c* at pH 1.5 as shown in panel a (■), and at pH 7 (○).

concentrations of urea these signals appear to merge with the post-unfolding baseline of the equilibrium unfolding transition recorded at pH 7. These observations indicate that the burst folding fluorescence of cyt *c* originates from the unfolded state of the protein under denaturant-diluted refolding conditions, and that the urea-dependence of burst signals represents most likely an extension of the postunfolding baseline to nativelike conditions rather than the titration of an early kinetic intermediate.

Testing on the Origin of GdnHCl Dependence of Burst Fluorescence of cyt c. Since GdnHCl is more relevant for kinetic studies with cyt *c*, it is desirable to probe into GdnHCl dependence of burst fluorescence changes. The U_A state of ferricyt *c* (pH 2) was used for this set of experiments also. But U_A is known to assume a molten globule-like structure in the presence of increasing concentrations of GdnHCl up to ~1 M (*40*). A temperature melt of U_A in the presence of 0.9 M GdnHCl (data not shown) suggested that it is largely unstructured at temperatures >40 °C. The effect of GdnHCl on fluorescence signals of the U_A state was therefore studied at 42 (±2) °C. Experiments involved measurement of (i) equilibrium fluorescence of U_A as a function of GdnHCl,

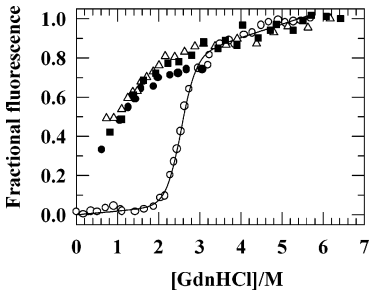

FIGURE 6: GdnHCl dependence of burst signals of ferricyt *c* obtained from stopped-flow dilution of GdnHCl at pH 2, 42 (±2) °C (Δ) and at pH 7, 10 °C (●) are compared with the equilibrium fluorescence of the protein at pH 2, 42 (±2) °C (■) and at pH 7, 10 °C. Equilibrium unfolding transition at pH 7, 10 °C (○) is also plotted. The fit to the normal unfolding transition yields ΔG°_D = 7.94 kcal mol^{-1}, and m_g = 3.16 kcal mol^{-1} M^{-1}.

(ii) burst change in fluorescence of U_A in stopped-flow GdnHCl jumps, (iii) equilibrium unfolding of ferricyt *c* at 10 and 40 °C, pH 7, and (iv) stopped-flow refolding kinetics at 10 °C, pH 7.

Figure 6 shows the pertinent data. The equilibrium fluorescence of cyt *c* at pH 2 (U_A), and the $t = 0$ fluorescence signals determined from kinetic experiments at pH 2 (U_A) and at pH 7, all show the same dependence on GdnHCl within the limitations of experimental constraints (see the figure legend), and these three sets of fluorescence values merge with the postunfolding baseline of the GdnHCl-induced transition of cyt *c* (pH 7). Thus, the GdnHCl distribution of burst signals recorded in normal refolding experiments may be taken as the extension of the post-unfolding baseline to nativelike conditions. These results again indicate that the burst fluorescence of cyt *c* is due to the transient denatured state generated when the denaturant is diluted rapidly to drive the protein to fold.

DISCUSSION

Since the unfolded polypeptide cannot sample out the possible configurations within the Levinthal limit of even the smallest of all real proteins, it is generally believed that folding is hierarchic, and progresses through discrete pathways consisting of one or more intermediates (*42*). Possible kinetic intermediates most often escape detection, and are not amenable to structural characterization due to their transient lifetime and accumulation to an insufficient level. Kinetic folding intermediates are described best if their equilibrium accumulation is demonstrated. Implication of one or more intermediates in both equilibrium and kinetic processes would, therefore, strengthen the pathway concept of folding.

Two-State Equilibrium of Ferrocyt c at Neutral pH. A part of the present study concerns whether structural intermediates accumulate to a level detectable at neutral pH in the equilibrium unfolding of ferrocyt *c*. The basic experimental test to ascertain the operation of a protein according to the two-state equilibrium, N ⇌ U, is the coincidence of unfolding transitions for multiple spectroscopic probes (*43*), although observation of distinct transition curves of two different properties for the denaturation does not necessarily provide a proof of the existence of an intermediate (*44*). By this criterion (Figure 1), no structural intermediate of substantial thermodynamic stability populates across the unfolding

transition of ferrocyt *c*. Another evidence for the N ⇌ U equilibrium is found from the ratio of calorimetric to effective enthalpies at various transition temperatures. Although horse ferrocyt *c* is not directly amenable to the usual thermal unfolding studies due to its unusually large conformational stability, extensive calorimetric studies of Privalov and co-workers (*45*, *46*) with oxidized cyt *c* have indicated many years ago that the ratio of calorimetric enthalpy to van't Hoff enthalpy is close to unity, suggesting the existence of insignificant populations of intermediates that are thermodynamically stable. It is noted that thermal reversibility and calorimetric data for yeast iso-1 and iso-2 ferrocyt *c* have been reported (*47*, *48*).

The tests conducted here thus provide no evidence for a neutral-pH equilibrium intermediate of horse cyt *c*. Well-defined equilibrium intermediate at physiological pH for proteins the size of cyt *c* or smaller has been rarely described. In fact, to a very good approximation, unfolding transitions of small globular proteins are representatives of a cooperative two-state transition (*45*). On the other hand, the accumulation of detectable intermediates in equilibrium transitions of proteins relatively larger or moderate in size has been shown many years ago in several cases, including α-lactalbumin (*49*, *50*), chicken cystatin (*51*), pituitary growth hormone (*52*), bovine carbonic anhydrase (*53*), penicillinase (*54*), and disulfide isomerase (*55*). Two-state transition of small proteins at physiological pH could be a consequence of their size, and the lack of disulfides or interactions essential for stabilization of intermediates. Stabilizing interactions, introduced by adding ions for eliminating charge−charge repulsions in acid or alkaline solutions, for example, lead to accumulation of partly folded conformations. For ferricyt *c*, the formation of a molten globule at pH ∼ 2 and high salt, also called the "A state", has been well documented (*41*, *56*−*58*). Demonstration of the possible existence of the acid molten globule of ferrocytchrome *c* has not been possible due to severe experimental constraints imposed by the higher autoxidation rate of the protein at acid pH.

Origin and Interpretation of Curved Chevron Plot of Ferrocytochrome c. The idea that the downward curvature in the folding limb of chevron plots could be related to transient accumulation of sub-millisecond folding intermediates is due to the early work of Fersht and co-workers with barnase (*20*). The implication of folding intermediates in chevron curvatures received major support from observations that a sizable set of proteins whose refolding rates roll over under nativelike conditions also display varying degrees of loss of optical signals in a burst refolding phase. Mainly on the basis of these facts, it has been generalized that chevron curvatures reflect accumulation of folding intermediates (*22*). It is a general belief that the stopped-flow rates roll over because the burst product limits the overall rate of folding to the native state. The rollover is accentuated with increasing stabilization, and therefore accumulation, of the burst product as more nativelike conditions are approached. As such, this interpretation appears rational. However, chevron curvature is also seen in the unfolding limb of ferrocyt *c* (Figure 3b), even though no burst unfolding signal is recorded (Figure 3c). Further, loss of optical signals in the sub-millisecond regime need not necessarily mean accumulation of an intermediate. Assignment of the burst product to a structural intermediate requires knowledge of its attribute. It is therefore necessary to analyze in detail the chevron properties and denaturant dependences of burst optical signals.

A subset of refolding experiments, where kinetics of folding of the GdnHCl-unfolded protein to different final concentrations of GdnHCl are recorded as a function of a weaker denaturant like urea (Figure 4b), provide some clues to chevron curvature. The parameter of main interest is $m_f^{\ddagger}$ that provides a measure of surface area that is buried in going from the U′ state to the transition state, ‡, (*42*) according to the following scheme

$$U \rightarrow U' \rightarrow \ddagger \rightarrow N$$

U′ forms incipiently when the denaturant is diluted out and is the initial denatured protein or an early folding intermediate, depending on the extent of its structure. Within error, the same value of $m_f^{\ddagger}$ is obtained for different concentrations of GdnHCl. This result is not expected if the attribute of U′ is a structural intermediate. If it were so, the value of $m_f^{\ddagger}$ obtained from rate-urea space for a low GdnHCl concentration (0.9 M) that strongly supports structure would have been different from that for a higher concentration of GdnHCl (3.0 M) where intermediates are not expected to accumulate. According to this interpretation, the folding transition state of ferrocytochrome *c* is largely immobile.

Chevron curvature in other two-state proteins has been explained by assuming mobile transition states (ref *37*, for example). Movement of the transition state ensemble toward the unfolded state under conditions of increased protein stability is envisaged if Hammond behavior is invoked (*59*, *60*). According to this model, a broad energy barrier separates the native state from the unfolded one. The rate-limiting transition state ensemble which is the highest point on the barrier energy profile moves toward the unfolded state upon approaching nativelike conditions, giving rise to rate rollover in the refolding limb of the chevron. Similarly, movement of the rate-limiting ensemble toward the native state at high denaturant concentrations can cause a curvature in the unfolding limb of the chevron. This model was used to explain the curvatures in both folding and unfolding limbs of the chevron plot of the two-state protein U1A (*37*).

Chevron rollover in the absence of kinetic intermediates can also be explained by invoking a continuum of rapidly inteconverting collapsed states such that the rates of interconversion are irresolvable in the time-scale of conversion of each individual collapsed state to the native state (*61*). Denaturant-dependent redistribution of the collapsed ensemble may give rise to rate rollover. The continuum model was used to explain the chevron curvature for half a dozen proteins (*61*).

These alternative interpretations of chevron curvature are context specific. They do not anull the interpretation relating to the accumulation of kinetic intermediates. To make further progress, the nature of the burst product the accumulation of which supposedly gives rise to curvatures needs to be ascertained.

Possible Origin of Burst Refolding Phase of cyt c. Both dimensional and configurational properties of denatured proteins are highly sensitive to changing solvent conditions. The density of unfolded chains, for example, increases linearly as the ionic strength of the denaturing medium increases (*44*). Similarly, polypeptide chains expand as the

solvent quality becomes better but contract when diluted into a poorer solvent that supports folding. Non-native states are also characterized by ultrafast reorganization of backbone dihedral angles at the level of individual residues (*62*) and the average distribution of $\phi-\psi$ angles across the backbone changes in a solvent-specific manner (*62*, *63*). These solvent-dependent chain geometries are known to generate optical activity not bona fide to extended secondary structural elements that characterize native or nativelike structures (*64*). Solvent dependent chain contraction or expansion also alters fluorescence and extinction coefficients of chromophores depending on the extent of readjustments in their spatial locations and environments. The stopped-flow burst signals that are produced in response to a transfer of the unfolded polypeptide from higher to lower concentrations of a denaturant must then be considered from this perspective.

That burst signals in stopped-flow refolding experiments could be due to a fast contraction of the polypeptide and readjustments of the average backbone geometry was first suggested by Sosnick et al. (*38*). By modeling two large unstructured peptide fragments of cyt *c* (F1−65 and F1−80) for the unfolded protein they found that burst changes in both fluorescence and CD signals recorded in normal refolding experiments with holocyt *c* are quantitatively identical with the corresponding signals for the unfolded protein. The same conclusion was reached with Rnase A (*39*). They suggested that the product of the sub-millisecond burst phase is simply the transient unfolded state under low GdnHCl refolding condition where both geometry and dimension of the polypeptide readjust to the new solvent milieu. Hence, the burst signals are due to the overall response of the unfolded polypeptide under the new solvent conditions rather than to a structured intermediate. This conclusion was found inconsistent with the real-time partial resolution of the burst phase as an exponential process characterized by a modest energy barrier between the initial unfolded state and the burst product (*5*). Accordingly, it has been argued that the burst signals originate from a specific process whereby the unfolded state collapses to a structured intermediate. There have also been concerns whether the fragments of cyt *c* missing as much as a third of the protein and ∼45% of the hydrophobic side-chains can be considered as representative models for the denatured state of the whole protein (*22*).

Results show that both equilibrium and kinetic burst fluorescence signals of the intact and unstructured cyt *c* under persisting unfolding conditions vary with denaturant in a quantitatively identical manner with the denaturant dependence burst amplitudes recorded in normal refolding kinetics of cyt *c* at pH 7. Further, as Figures 5 and 6 show, the phenomenon is observed with both GdnHCl and urea, suggesting that the submillisecond process is associated with a U → U′ process where U′ is the unfolded state under refolding conditions. Identical results are obtained when these experiments are repeated with CD (data not shown). More direct evidence for the lack of extended secondary structure in the collapsed U′ state comes from CD-monitored real-time sub-millisecond kinetics of cyt *c* refolding. The data of Akiyama et al. (*65*) show that the helix content in the burst product is some 8% of that in native cyt *c*. A further analysis of their data has shown that the burst CD amplitude closely matches the equilibrium CD signal of unfolded cyt *c* (*66*).

Since the objective of the present study is to examine the refolding kinetics of ferrocytochrome *c*, it is desirable to interrogate the burst phenomenon directly on the reduced state of the protein, even though the heme oxidation state of the same protein is not expected to make a great difference in the early collapse. Unfortunately, due to both very high aqueous stability and enhanced autoxidation rate at lower pH, a solvent condition in which ferrocyt *c* can be held unfolded steadily is hard to find. Nevertheless, a CD-monitored ultrafast refolding study shows that the unstructured attribute of the burst product is true for ferrocyt *c* as well. Chen et al. (*67*) triggered refolding of ferrocyt *c* in the presence of 3.5 M GdnHCl, a solvent condition in which ferricyt *c* is largely unfolded but ferrocyt *c* is completely native, by photoinduced electron transfer from NADH to the oxidized protein. Using time-resolved CD spectroscopy they found that just about 20% of the total expected ellipticity in the far-UV region is recovered in the sub-millisecond regime. Actually, the number would be much smaller than 20% when the allowance for some residual helicity of oxidized cyt *c* in the presence of 3.5 M GdnHCl is given.

Two-State Folding Kinetics of Ferrocytochrome c. The results and interpretations presented weigh in rather substantially toward the view that chevron rollover in ferrocyt *c* (Figure 3b) is inconsistent with accumulation of a folding intermediate. This conclusion is further supported by observations that the burst phase represents the earliest collapse of the unfolded state to a state (U′) that is devoid of any considerable nativelike structure. These derivations constrain the folding mechanism of ferrocyt *c* to the simple U → U′ → N scheme, where U → U′ represents the unobservable sub-millisecond relaxation of the unfolded state, and the U′ → N is the stopped-flow observable single-exponential refolding. The folding kinetics is, therefore, effectively two-state. With this background the following paper in this issue uses additional data on ferrocyt *c* to examine the self-sufficiency of the classical folding model.

ACKNOWLEDGMENT

We gratefully acknowledge many helpful suggestions and support of Jayant B. Udgaonkar. A.K.B. is the recipient of a Swarnajayanti Fellowship from the Department of Science & Technology, Government of India.

REFERENCES

1. Ikai, A., Fish, W. W., and Tanford, C. (1973) Kinetics of unfolding and refolding of proteins II. Results for cytochrome *c*, *J. Mol. Biol. 73*, 165−184.
2. Knapp, J. A., and Pace, C. N. (1974) Guanidine hydrochloride and acid denaturation of horse, cow, and *Candida krusei* cytochrome *c*, *Biochemistry 13*, 1289−1294.
3. Privalov, P. L., and Khechinashvili, N. N. (1974) A thermodynamic approach to the problem of stabilization of globular protein structure: A calorimetric study, *J. Mol. Biol. 86*, 665−684.
4. Tsong, T. Y. (1974) The Trp-59 fluorescence of ferricytochrome *c* as a sensitive measure of the overall protein conformation, *J. Biol. Chem. 249*, 1988−1990.
5. Shastry, M. C. R., Sauder, J. M., and Roder, H. (1998) Kinetic and structural analysis of submillisecond folding events in cytochrome *c*, *Acc. Chem. Res. 31*, 717−725.
6. Yeh, S.-R., Han, S., and Rousseau, D. L. (1998) Cytochrome *c* folding and unfolding: a biphasic mechanism, *Acc. Chem. Res. 31*, 727−736.

7. Englander, S. W., Sosnick, T. R., Mayne, L. C., Shtilerman, M., Qi, P. X., and Bai, Y. (1998) Fast and slow folding in cytochrome *c*, *Acc. Chem. Res. 31*, 737−744.
8. Krishna, M. M. G., Lin, Y., Rumbley, J. N., and Englander, S. W. (2003) Cooperative omega loops in cytochrome *c*: role in folding and function, *J. Mol. Biol. 331*, 29−36.
9. Muthukrishnan, K., and Nall, B. T. (1991) Effective concentrations of amino acid side-chains in an unfolded protein, *Biochemistry 30*, 4706−4710.
10. Sosnick, T. R., Mayne, L., Hiller, R., and Englander, S. W. (1994) The barriers in protein folding, *Nat. Struct. Biol. 1*, 149−156.
11. Elöve, G. A., Bhuyan, A. K., and Roder, H. (1994). Kinetic mechanism of cytochrome *c* folding: involvement of the heme and its ligands, *Biochemistry 33*, 6925−6935.
12. Bhuyan, A. K., and Kumar, R. (2002) Kinetic barriers to the folding of horse cytochrome *c* in the reduced state, *Biochemistry 41*, 12821−12834.
13. Wolynes, P. G., Onuchic, J. N., and Thirumalai, D. (1995) Navigating the folding routes, *Science 267*, 1619−1620.
14. Colón, W., Elöve, G. A., Wakem, L. P., Sherman, F., and Roder, H. (1996) Side-chain packing of the N- and C-terminal helices plays a critical role in the kinetics of cytochrome *c* folding, *Biochemistry 35*, 5538−5549.
15. Sosnick, T. R., Mayne, L., and Englander, S. W. (1996) Molecular collapse: the rate-limiting step in two-state cytochrome *c* folding, *Proteins 24*, 413−426.
16. Bhuyan, A. K., and Udgaonkar, J. B. (2001) Folding of horse cytochrome *c* in the reduced state, *J. Mol. Biol. 312*, 1135−1160.
17. Prabhu, N. P., Kumar, R., and Bhuyan, A. K. (2004) Folding barrier in horse cytochrome *c*: support for a classical folding pathway, *J. Mol. Biol. 337*, 195−208.
18. Kumar, R., Prabhu, N. P., Yadaiah, M., and Bhuyan, A. K. (2004) Protein stiffening and entropic stabilization in the subdenaturing limit of guanidine hydrochloride, *Biophys. J. 87*, 2656−2662.
19. Pabit, S. A., Roder, H., and Hagen, S. J. (2004) Internal friction controls the speed of protein folding from a compact configuration, *Biochemistry 43*, 12532−12538.
20. Matouschek, A., Kellis, J. T., Jr., Serrano, L., Bycroft, M., and Fersht, A. R. (1990) Transient folding intermediates characterized by protein engineering, *Nature 346*, 440−445.
21. Baldwin, R. L. (1996) On-pathway versus off-pathway folding intermediates, *Folding Des. 1*, R1−R8.
22. Roder, H., and Colón, W. (1997) Kinetic role of early intermediates in protein folding, *Curr. Opin. Struct. Biol. 7*, 15−28.
23. Park, S. H., Shastry, M. C, and Roder, H. (1999) Folding dynamics of the B1 domain of protein G explored by ultrarapid mixing, *Nat. Struct. Biol. 6*, 943−947.
24. Maki, K., Cheng, H., Dolgikh, D. A., Shastry, M. C., and Roder, H. (2004) Early events during folding of wild-type staphylococcal nuclease and a single-tryptophan variant studied by ultrarapid mixing, *J. Mol. Biol. 338*, 383−400.
25. McCallister, E. L., Alm, E., and Baker, D. (2000) Critical role of beta-hairpin formation in protein G folding, *Nat. Struct. Biol. 7*, 669−673.
26. Takei, J., Chu, R.-A., and Bai, Y. (2000) Absence of stable intermediates on the folding pathway of barnase, *Proc. Natl. Acad. Sci. U.S.A. 97*, 10796−10801.
27. Krantz, B. A., and Sosnick, T. R. (2000) Distinguishing between two-state and three-state models for ubiquitin folding, *Biochemistry 39*, 11696−11701.
28. Parker, M. J., and Marqusee, S. (2001) A kinetic folding intermediate probed by native state hydrogen exchange, *J. Mol. Biol. 305*, 593−602.
29. Jacob, J., Krantz, B., Dothager, R. S., Thiyagarajan, P., and Sosnick, T. R. (2004) Early collapse is not an obligate step in protein folding, *J. Mol. Biol. 338*, 369−382.
30. Bhuyan, A. K., Rao, D. K., and Prabhu, N. P. (2005) Protein folding in classical perspective: folding of horse cytochrome *c*, *Biochemistry*, *44*, xxx−xxx.
31. Tanford, C. (1970) Protein denaturation. C. Theoretical models for the mechanism of denaturation, *Adv. Protein. Chem. 24*, 1−95.
32. Pace, C. N. (1986) Determination and analysis of urea and guanidine hydrochloride denaturation curves, *Methods Enzymol. 131*, 266−280.
33. Filmonov, V. V., and Rogov, V. V. (1996) Reversible association of the equilibrium unfolding intermediate of lambda *Cro* repressor, *J. Mol. Biol. 255*, 767−777.
34. Semisotnov, G. V., Kihara, H., Kotova, N. N., Kimura, K., Amemiya, Y., Wakabayashi, K., Serdyuk, I. N., Timchenko, A. A., Chiba, K., Nikaido, K., Ikura, T., and Kuwajima, K. (1996) Protein globularization during folding. A study by synchrotron small-angle X-ray scattering, *J. Mol. Biol. 262*, 559−574.
35. Gupta, R., and Ahmad, F. (1999) Protein Stability: functional dependence of denaturational Gibbs energy on urea concentration, *Biochemistry 38*, 2471−2479.
36. Santoro, M. M., and Bolen, D. W. (1988) Unfolding free energy changes determined by the linear extrapolation method. 1. Unfolding of phenylmethanesulfonyl alpha-chymotrypsin using different denaturants, *Biochemistry 27*, 8063−8068.
37. Otzen, D. E., Kristensen, O., Proctor, M., and Oliveberg, M. (1999) Structural changes in the transition state of protein folding: alternative interpretations of curved chevron plots, *Biochemistry 38*, 6499−6511.
38. Sosnick, T. R., Shtilerman, M. D., Mayne, L., and Englander, S. W. (1997) Ultrafast signals in protein folding and the polypeptide contracted state, *Proc. Natl. Acad. Sci. U.S.A. 94*, 8545−8550.
39. Qi, P. Q., Sosnick, T. R., and Englander, S. W. (1998) The burst phase in ribonuclease A folding: solvent dependence of the unfolded state, *Nat. Struct. Biol. 5*, 882−884.
40. Hagihara, Y., Aimoto, S., Fink, A. L., and Goto, Y. J. (1993) Guanidine hydrochloride-induced folding of proteins, *J. Mol. Biol. 231*, 180−184.
41. Jeng, M. F., and Englander, S. W. (1991) Stable submolecular folding units in a non-compact form of cytochrome *c*, *J. Mol. Biol. 221*, 1045−1061.
42. Baldwin, R. L., and Rose, G. D. (1999) Is protein folding hierarchic? II. Folding intermediates and transition states, *Trends Biochem. Sci. 24*, 77−83.
43. Thomson, J. A., Shirley, B. A., Grimsley, G. R., and Pace, C N. (1989) Conformational stability and mechanism of folding of ribonuclase T1, *J. Biol. Chem. 264*, 11614−11620.
44. Dill, K. A., and Shortle, D. (1991) Denatured states of proteins, *Annu. Rev. Biochem. 60*, 795−825.
45. Privalov, P. L. (1979) Stability of proteins: small globular proteins, *Adv. Protein Chem. 33*, 167−241.
46. Privalov, P. L., and Khechinashvili, N. N. (1974) A thermodynamic approach to the problem of stabilization of globular protein structure: a calorimetric study, *J. Mol. Biol. 86*, 665−684.
47. Cohen, D. S., and Pielak, G. J. (1995) Entropic stabilization of cytochrome *c* upon reduction, *J. Am. Chem. Soc. 117*, 1675−1677.
48. McGee, W. A., Rosell, F. I., Liggins, J. R., Rodriguez-Ghidarpour, S., Luo, Y., Chen, J., Brayer, G. D., Mauk, A. G., and Nall, B. T. (1996) Thermodynamic cycles as probes of structure in unfolded proteins, *Biochemistry 35*, 1995−2007.
49. Kuwajima, K., Nitta, K., Yoneyama, M., and Sugai, S. (1976) Three-state denaturation of alpha-lacalbumin by guanidine hydrochloride, *J. Mol. Biol. 106*, 359−373.
50. Kuwajima, K. (1977) A folding model of alpha-lactalbumin deduced from the three-state denaturant mechanism, *J. Mol. Biol. 114*, 241−258.
51. Bjork, I., and Pol, E. (1992) Biphasic transition curve on denaturation of chicken cystatin by guanidinium chloride. Evidence for an independently unfolding structural region, *FEBS Lett. 299*, 66−68.
52. Holladay, L. A., Hammonds, R. G., and Puett, D. (1974) Growth hormone conformation and conformational equilibria, *Biochemistry 13*, 1653−1661.
53. Wong, K.-P., and Tanford, C. (1973) Denaturation of bovine carbonic anhydrase B by guanidine hydrochloride. A process involving separable sequential conformational transitions. *J. Biol. Chem. 248*, 8518−8523.
54. Robson, I., and Pain, R. H. (1976) The mechanism of folding of globular proteins. Equilibrium and kinetics of conformational transitions of penicillinase from Staphylococcus aureus involving a state of intermediate conformation, *Biochem J. 155*, 331−344.
55. Morjana, N. A., McKeone, B. J., and Gilbert, H. F. (1993) Guanidine hydrochloride stabilization of a partially unfolded intermediate during the reversible denaturation of protein disulfide isomerase, *Proc. Natl. Acad. Sci. U.S.A. 90*, 2107−2111.
56. Ohgushi, M., and Wada, A. (1983) 'Molten-globule state': a compact form of globular proteins with mobile side-chains, *FEBS Lett. 164*, 21−24.
57. Goto, Y., Takahashi, N., and Fink, A. L. (1990) Mechanism of acid-induced folding of proteins, *Biochemistry 29*, 3480−3488.
58. Jeng, M.-F., Englander, S. W., Elöve, G. A., Wand, A. J., and Roder, H. (1990) Structural description of acid-denatured cyto-

chrome *c* by hydrogen exchange and 2D NMR, *Biochemistry 29*, 10433−10437.
59. Matouschek, A., and Fersht, A. R. (1993) Application of physical organic chemistry to engineered mutants of proteins: Hammond postulate behavior in the transition state of protein folding, *Proc. Natl. Acad. Sci. U.S.A. 90*, 7814−7818.
60. Matthews, J. M., and Fersht, A. R. (1995) Exploring the energy surface of protein folding by structure−reactivity relationships and engineered proteins: observation of Hammond behavior for the gross structure of the transition state and anti-Hammond behavior for structural elements for unfolding/folding of barnase, *Biochemistry 34*, 6805−6810.
61. Parker, M. J., and Marqusee, S. (1999) The cooperativity of burst phase reactions explored, *J. Mol. Biol. 293*, 1195−1210.
62. Barron, L. D., Hecht, L., and Wilson, G. (1997) The lubricant of life: a proposal that solvent water promotes extremely fast conformational fluctuations in mobile heteropolypeptide structure, *Biochemistry 36*, 13143−13147.
63. Park, S.-H., Shalongo, W., and Stellwagen, E. (1997) The role of PII conformation in the calculation of peptide fractional helix content, *Protein Sci. 6*, 1694−1700.
64. Wilson, G., Hecht, L., and Barron, L. D. (1996) Residual structure in unfolded proteins revealed by Raman Optical Activity, *Biochemistry 35*, 12518−12525.
65. Akiyama, S., Takahashi, S., Ishimori, K., and Morishima, I. (2000) Stepwise formation of α-helices during cytochrome *c* folding, *Nat. Struct. Biol. 7*, 514−520.
66. Krantz, B. A., Mayne, L., Rumbley, J., Englander, S. W., and Sosnick, T. R. (2002) Fast and slow intermediate accumulation and the initial barrier mechanism in protein folding, *J. Mol. Biol. 234*, 359−371.
67. Chen, E., Wittung-Stafshede, P., and Kliger, D. S. (1999) Far-UV time-resolved circular dichroism detection of electron-transfer-triggered cytochrome *c* folding, *J. Am. Chem. Soc. 121*, 3811−3817.

BI0478998